




Transcriptomic analysis of the gonads of *Locusta migratoria* (Orthoptera: Acrididae) following infection with *Paranosema locustae*

Xuwei Kong^{1,2}, Xinrui Guo^{1,2}, Jun Lin³, Hui Liu^{1,2}, Huihui Zhang^{1,2}, Hongxia Hu^{1,2}, Wangpeng Shi⁴, Rong Ji^{1,2}, Roman Jashenko⁵ and Han Wang^{1,2} 

Research Paper

Cite this article: Kong X *et al* (2024). Transcriptomic analysis of the gonads of *Locusta migratoria* (Orthoptera: Acrididae) following infection with *Paranosema locustae*. *Bulletin of Entomological Research* 1–13. <https://doi.org/10.1017/S0007485324000592>

Received: 6 June 2024
Revised: 13 August 2024
Accepted: 20 September 2024

Keywords:
Locusta migratoria; ovary; *Paranosema locustae*; testis; transcriptome

Corresponding author:
Han Wang;
Email: 78984935@qq.com

¹International Research Center for the Collaborative Containment of Cross-Border Pests in Central Asia, Xinjiang Key Laboratory of Special Species Conservation and Regulatory Biology, College of Life Sciences, Xinjiang Normal University, Urumqi 830054, China; ²Tacheng, Research Field (Migratory Biology), Observation and Research Station of Xinjiang, Tacheng 834700, China; ³Central for Prevention and Control of Prediction & Forecast Prevention of Locust and Rodent, Xinjiang Uygur Autonomous Region, China; ⁴College of Plant Protection, China Agricultural University, Beijing 100193, China and ⁵Ministry of Education and Science of the Republic of Kazakhstan, Almaty 050060, Kazakhstan

Abstract

Paranosema locustae is an environmentally friendly parasitic predator with promising applications in locust control. In this study, transcriptome sequencing was conducted on gonadal tissues of *Locusta migratoria* males and females infected and uninfected with *P. locustae* at different developmental stages. A total of 18,635 differentially expressed genes (DEGs) were identified in female ovary tissue transcriptomes, with the highest number of DEGs observed at 1 day post-eclosion (7141). In male testis tissue transcriptomes, a total of 32,954 DEGs were identified, with the highest number observed at 9 days post-eclosion (11,245). Venn analysis revealed 25 common DEGs among female groups and 205 common DEGs among male groups. Gene ontology and Kyoto Encyclopaedia of Genes and Genome analyses indicated that DEGs were mainly enriched in basic metabolism such as amino acid metabolism, carbohydrate metabolism, lipid metabolism, and immune response processes. Protein–protein interaction analysis results indicated that *L. migratoria* regulates the expression of immune- and reproductive-related genes to meet the body's demands in different developmental stages after *P. locustae* infection. Immune- and reproductive-related genes in *L. migratoria* gonadal tissue were screened based on database annotation information and relevant literature. Genes such as *Tsf*, *Hex1*, *Apolp-III*, *Serp*, *Def*, *Hsp70*, *Hsp90*, *JHBP*, *JHE*, *JHEH1*, *JHAMT*, and *VgR* play important roles in the balance between immune response and reproduction in gonadal tissues. For transcriptome validation, *Tsf*, *Hex1*, and *ApoLp-III* were selected and verified by quantitative real-time polymerase chain reaction (qRT-PCR). Correlation analysis revealed that the qRT-PCR expression patterns were consistent with the RNA-Seq results. These findings contribute to further understanding the interaction mechanisms between locusts and *P. locustae*.

Introduction

Locusts are characterised by their gregarious behaviour, strong reproductive capacity, omnivorous diet, and strong migratory ability, causing severe damage to crops and grasslands, thereby posing a serious threat to food security and the healthy development of the ecological environment. Conducting scientifically effective comprehensive control measures is crucial. Chemical pesticide spraying is the primary method for locust control, particularly effective in controlling migratory and outbreak locust plagues. However, it often leads to serious issues such as locust resistance, pesticide residues, and environmental pollution. Therefore, there is an urgent need to find environmentally friendly, safe, and efficient pest control strategies.

Paranosema locustae is a single-celled eukaryotic organism that parasitises selectively on locusts and other orthopteran insects. It infects hosts and reproduces indefinitely, causing metabolic disorders, hindered organ development, reduced mobility, prolonged developmental periods, weakened reproductive capacity, and continuously spreads horizontally and vertically within locust populations, playing an important role in regulating locust population numbers (Zhang and Lecoq, 2021; Liu *et al.*, 2023; Zhang *et al.*, 2023a, 2023b). *P. locustae* exhibits high safety to non-orthopteran insects, vertebrates, and minimal environmental impact, thus becoming an important means of green locust control (Dakhel *et al.*, 2019; Chen *et al.*, 2020; Zhang and Lecoq, 2021).

To resist pathogen infections, locusts must invest a considerable amount of energy. However, limited energy intake cannot simultaneously meet the energy demands of immunity and reproduction. Therefore, there is a trade-off in resource allocation when organisms face stress (Schwenke, *et al.*, 2016; Budischak *et al.*, 2018; Shang *et al.*, 2018; Yao *et al.*, 2018).

© The Author(s), 2024. Published by Cambridge University Press. This is an Open Access article, distributed under the terms of the Creative Commons Attribution licence (<http://creativecommons.org/licenses/by/4.0/>), which permits unrestricted re-use, distribution and reproduction, provided the original article is properly cited.



Wang *et al.* (2019a) demonstrated that upon infection with *Micrococcus luteus*, genes such as *PPO1*, antimicrobial peptides, and defensins were upregulated, while *Vgs* expression levels were downregulated, indicating that locusts prioritise increasing investment in immune responses to maintain survival under *M. luteus* stress. *P. locustae* infection can induce immune response reactions in various host tissues, leading to increased immune investment and upregulation of immune-related gene expression. Lv *et al.* (2016) found that *P. locustae* infection induces the expression of defensins in *Locusta migratoria* fat bodies and salivary glands, but the transcription levels of defensins in fat bodies are lower, suggesting that *P. locustae* may weaken the immune response of fat bodies, making them more susceptible to infection. After *L. migratoria* infection with *P. locustae*, significant decreases in vitellogenin and vitellogenin receptor transcription expression, as well as reductions in vitellin content in fat bodies, haemolymph, and ovaries were observed, accompanied by significant decreases in egg cell number, ovarian length, and ovarian weight in female locusts, inhibiting vitellin deposition and ultimately reducing reproductive capacity (Chen *et al.*, 2002; Zhang and Lecoq, 2021; Hu *et al.*, 2022). Most studies imply that there is a mutual constraint between immunity and reproduction in the body after infection. The activation of immune responses leads to a diminished reproductive capacity.

Locusts possess strong reproductive abilities, which are the main reason for their outbreak. How do reproductive organs respond when the organism is under *P. locustae* infection stress? This study conducted transcriptome sequencing on gonadal tissues of *L. migratoria* males and females infected and uninfected with *P. locustae* at different developmental stages, analysed relevant bioinformatics data, and identified key genes and metabolic pathways involved in the balance between immunity and reproduction in *L. migratoria* gonadal tissues. This research provides data support for exploring the molecular biology mechanisms of interaction between *P. locustae* and locusts, screening optimal pest control targets, and further improving pest control effectiveness.

Materials and methods

Insect sources

L. migratoria eggs obtained from laboratory breeding were incubated in an artificial breeding chamber under the following conditions: temperature at $30 \pm 1^\circ\text{C}$, humidity at $50 \pm 5\%$, and a light–dark cycle of 14 L:10 D. After hatching, locust nymphs were reared to adulthood under the aforementioned conditions.

P. locustae infection

P. locustae provided by China Agricultural University was stored at -20°C . Based on preliminary trial results, each *L. migratoria* was infected with 1×10^4 spores of *P. locustae*. *L. migratoria* third-instar nymphs were infected using an individual feeding method (Panek *et al.*, 2014). Infected third-instar nymphs were reared to adulthood under the conditions mentioned in the section ‘Insect sources’. Then testes/ovaries were collected at third-instar nymphs (1 day post-infection) and also 1, 9, and 19 days post-eclosion of adults. These tissues were placed in RNA preservation solution (Tiangen, Beijing, China) and stored at -80°C for transcriptome sequencing. Three replicates were set for each age group, totalling 48 samples. Uninfected nymphs served as the control group.

RNA extraction and transcriptome sequencing

Total RNA from each sample was extracted using Trizol (Invitrogen, USA), and residual genomic DNA was removed using DNase I (Takara, China). The quantity and quality of RNA samples were assessed using a Nano Drop spectrophotometer (Thermo Fisher Scientific, DE). Transcriptome sequencing was conducted by Beijing Novogene Company using Illumina sequencing technology.

Data quality control

The Illumina platform converts the sequenced image signals into text signals via CASAVA Base Calling and stores them as raw data in the fastq format. Clean reads were obtained by removing reads containing adapter, poly-N, and low-quality reads from raw data. At the same time, Q20, Q30, and GC (guanine deoxyribonucleotide and cytosine deoxyribonucleotide) content of the clean data were calculated. All the downstream analyses were based on the clean reads with high quality.

De novo transcriptome assembly and gene annotation

Trinity was used to assemble clean reads (Grabherr *et al.*, 2011). Corset (Davidson and Oshlack, 2014) was adopted to cluster the assembled contigs based on shared reads. The longest transcripts of each cluster were selected as unigenes, which were then annotated and applied for the following analyses. Gene function was annotated based on the following databases: Nr (NCBI non-redundant protein sequences), Nt (NCBI non-redundant nucleotide sequences), Pfam (Protein family), COG (Cluster of Orthologous Groups of proteins) and KOG (euKaryotic Orthologous Groups), Swiss-Prot (a manually annotated and reviewed protein sequence database), KEGG (Kyoto Encyclopaedia of Genes and Genome), and GO (Gene Ontology).

Screening and enrichment analysis of differentially expressed genes

FPKM values were calculated to represent gene expression levels (Trapnell *et al.*, 2010). DESeq2 was used to determine differences in gene expression levels between two groups (Love *et al.*, 2014), calculating *P*-values, performing multiple hypothesis testing correction (Benjamini–Hochberg), and obtaining false-discovery rates (represented as P_{adj}). Using $P_{\text{adj}} < 0.05$ and $|\log_2\text{FoldChange}| > 2$ as criteria for selecting differentially expressed genes (DEGs). DEGs were screened for CFn3 vs. TFn3 (third-instar female locusts in the control group vs. infected group), CF1 vs. TF1 (1-day-old female locusts in the control group vs. infected group), CF9 vs. TF9 (9-day-old female locusts in the control group vs. infected group), CF19 vs. TF19 (19-day-old female locusts in the control group vs. infected group), CMn3 vs. TMn3 (third-instar male locusts in the control group vs. infected group), CM1 vs. TM1 (1-day-old male locusts in the control group vs. infected group), CM9 vs. TM9 (9-day-old male locusts in the control group vs. infected group), and CM19 vs. TM19 (19-day-old male locusts in the control group vs. infected group). Goseq (Young *et al.*, 2010) and KOBAS (Mao *et al.*, 2005) were used for GO and KEGG annotation and functional enrichment analysis of DEGs, with $P_{\text{adj}} < 0.05$ as the significance enrichment threshold.

Table 1. Transcriptome assembly results for *L. migratoria*

Unigene length	Numbers of transcripts		Unigenes number of unigenes	
	Number	Percentage	Number	Percentage
301–500 bp	185,084	43.572	111,636	49.356
501–1000 bp	119,998	28.250	69,785	30.853
1001–2000 bp	64,479	15.179	27,451	12.136
>2000 bp	55,218	12.999	17,314	7.655
Min length	301		301	
Max length	29,051		29,051	
Mean length	1058		845	
Median length	561		505	
Total number	424,779		226,186	
Total length	449,388,090		191,233,766	
N50	1746		1088	
N90	413		382	

PPI network construction

We performed protein–protein interaction (PPI) network analysis of the DEGs using the STRING database to construct potential interactions of genes with interaction scores >0.15. Then the networks created by STRING were imported into Cytoscape (version 3.9.1) software for visualisation.

Expression analysis of gonadal tissue stress response-related genes

Three immune- and reproductive-related genes were validated by quantitative real-time polymerase chain reaction (qRT-PCR) using TB Green® Premix Ex Taq™ II (Takara, China), with *EF1α* as the reference gene. Each reaction system (20 µl) included 10 µl TB Green, 1.0 µl each of upstream and downstream primers (table S1), 1 µl cDNA template, and 7.0 µl double-distilled water. The reaction programme included pre-denaturation at 95°C for 2 min; followed by 40 cycles of denaturation at 95°C for 10 s, annealing at 60°C for 10 s, and extension at 72°C for 10 s; and a final melting curve stage. Three samples were selected for each age group, with each sample tested three times. The Ct values were collected after the reaction, and the relative

gene expression levels were calculated using the $2^{-\Delta\Delta Ct}$ method. Data were represented as mean ± standard error. Single-factor analysis of variance (ANOVA) was performed using Origin2022 software ($P < 0.05$).

Results and analysis

Quality assessment of sequencing results

Transcriptome sequencing of gonadal tissues of infected and uninfected *L. migratoria* males and females with *P. locustae* was conducted using the Illumina HiSeq™ 6000 sequencing platform. Clean data for each sample ranged from 5.8 to 6.7 Gb, with GC content between 37.77 and 47.33%, and Q20 and Q30 values ranging from 97.14 to 97.77 and 92.45 to 93.71, respectively. A total of 226,186 unigenes were obtained, with an average length of 845 bp and an N50 length of 1088 bp. Unigenes longer than 1 kb accounted for 19.791% of the total (table 1). The assembly quality of Trinity.fasta, unigene.fasta, and cluster.fasta was evaluated using BUSCO software. The results showed a level of 98.1, 93.2, and 93.2% completeness for Trinity, unigene, and cluster, respectively, indicating good assembly completeness and high accuracy, suitable for subsequent analysis (fig. S1).

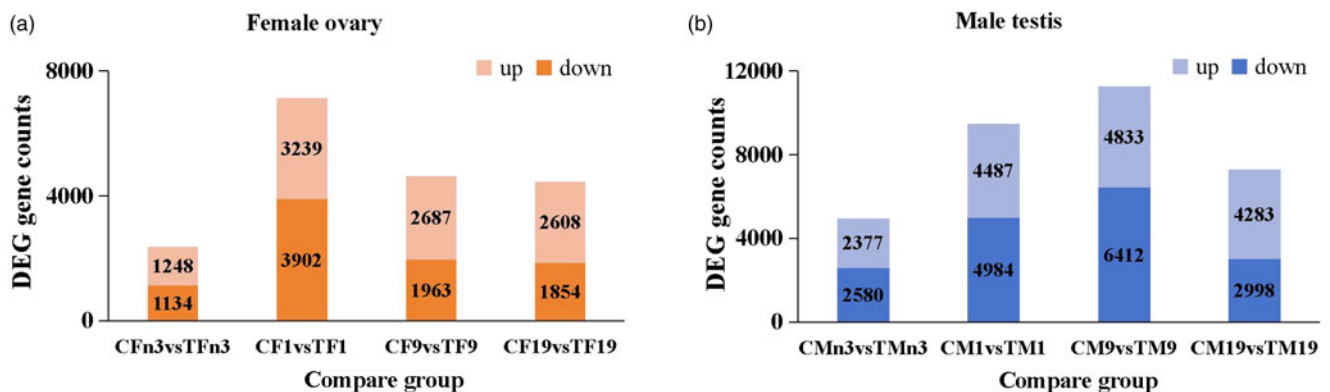


Figure 1. Histogram analysis of the number of DEGs between samples in ovary (A) and testis (B) of *L. migratoria*. After infection with *P. locustae*, ovary tissues of *L. migratoria* had the most DEGs at 1 day post-eclosion, while testis tissues had the most DEGs at 9 day post-eclosion.

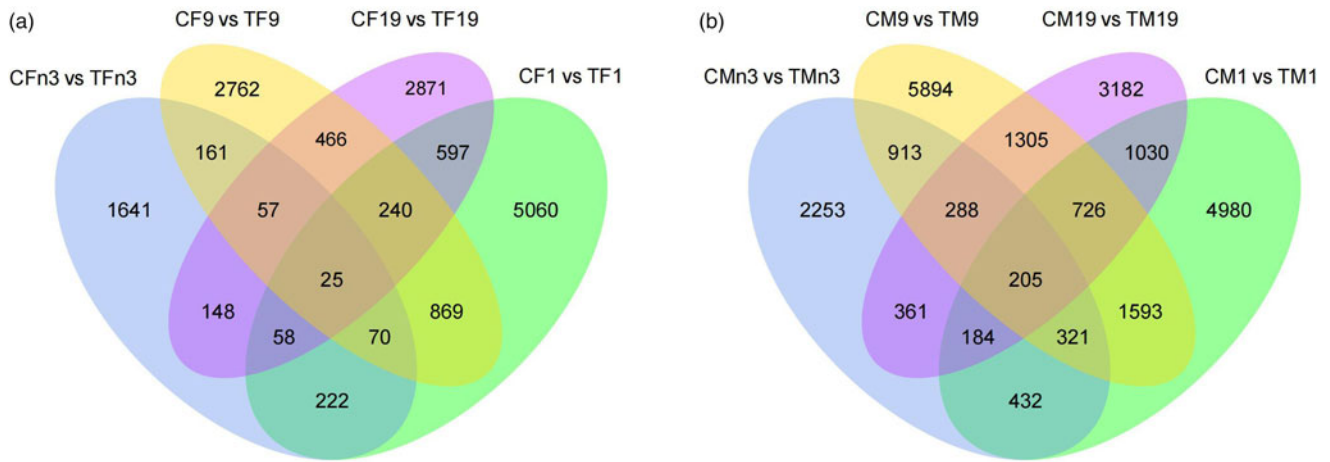


Figure 2. Venn diagrams analysis illustrated the overlap of DEGs among different comparison groups in ovary (A) and testis (B). After infection with *P. locustae*, there were 25 common DEGs in female ovary groups and 205 common DEGs in male testis groups.

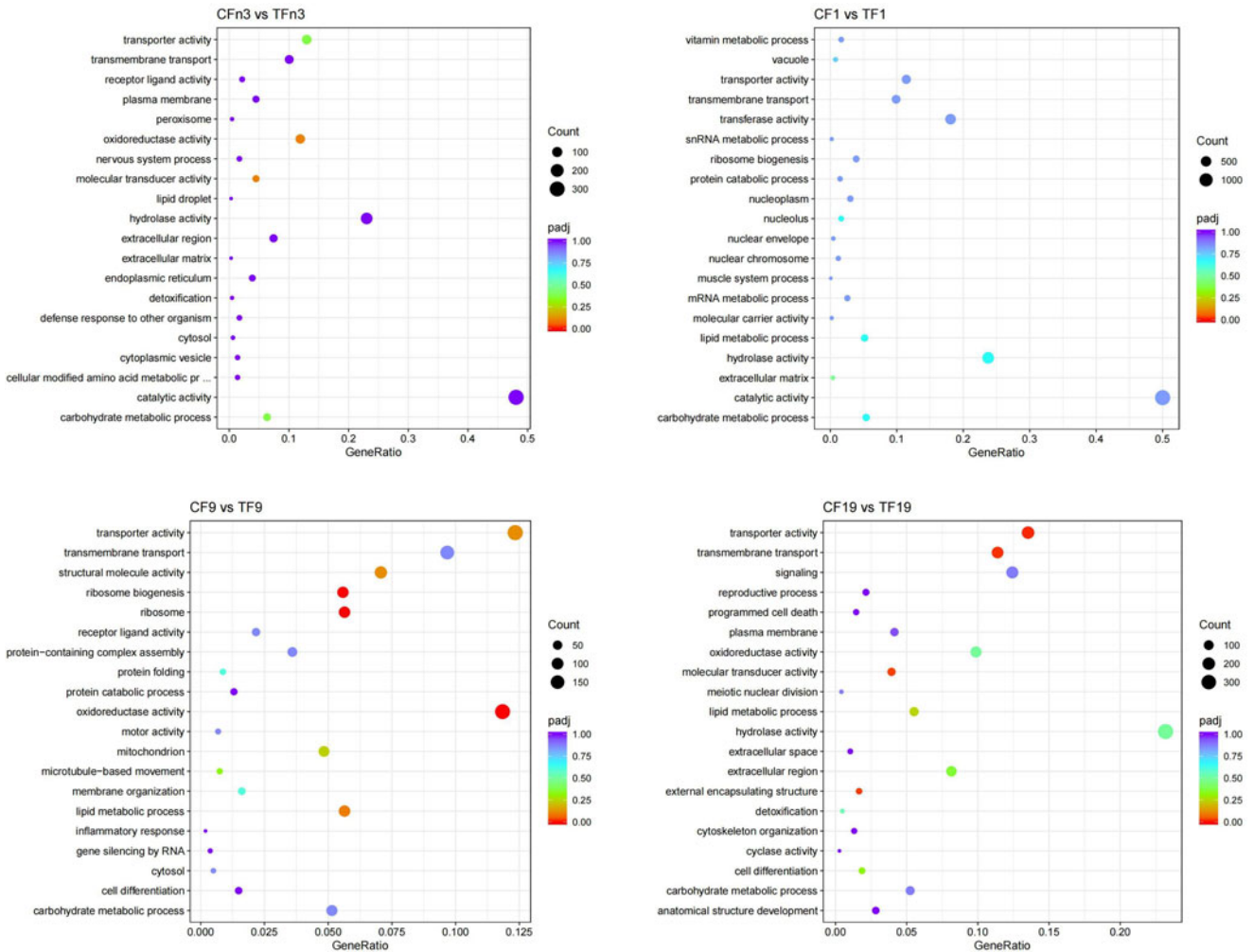


Figure 3. Dot plot of top 20 ranked GO terms of DEGs in different stages of female ovary of *L. migratoria*. The figures represent the CFn3 vs. TFn3, CF1 vs. TF1, CF9 vs. TF9, CF19 vs. TF19, respectively. The vertical axis indicates GO terms and the horizontal axis represents the gene ratio. The size of dots indicates the number of genes in the GO term, and the colour of the dots corresponds to different P_{adj} ranges.

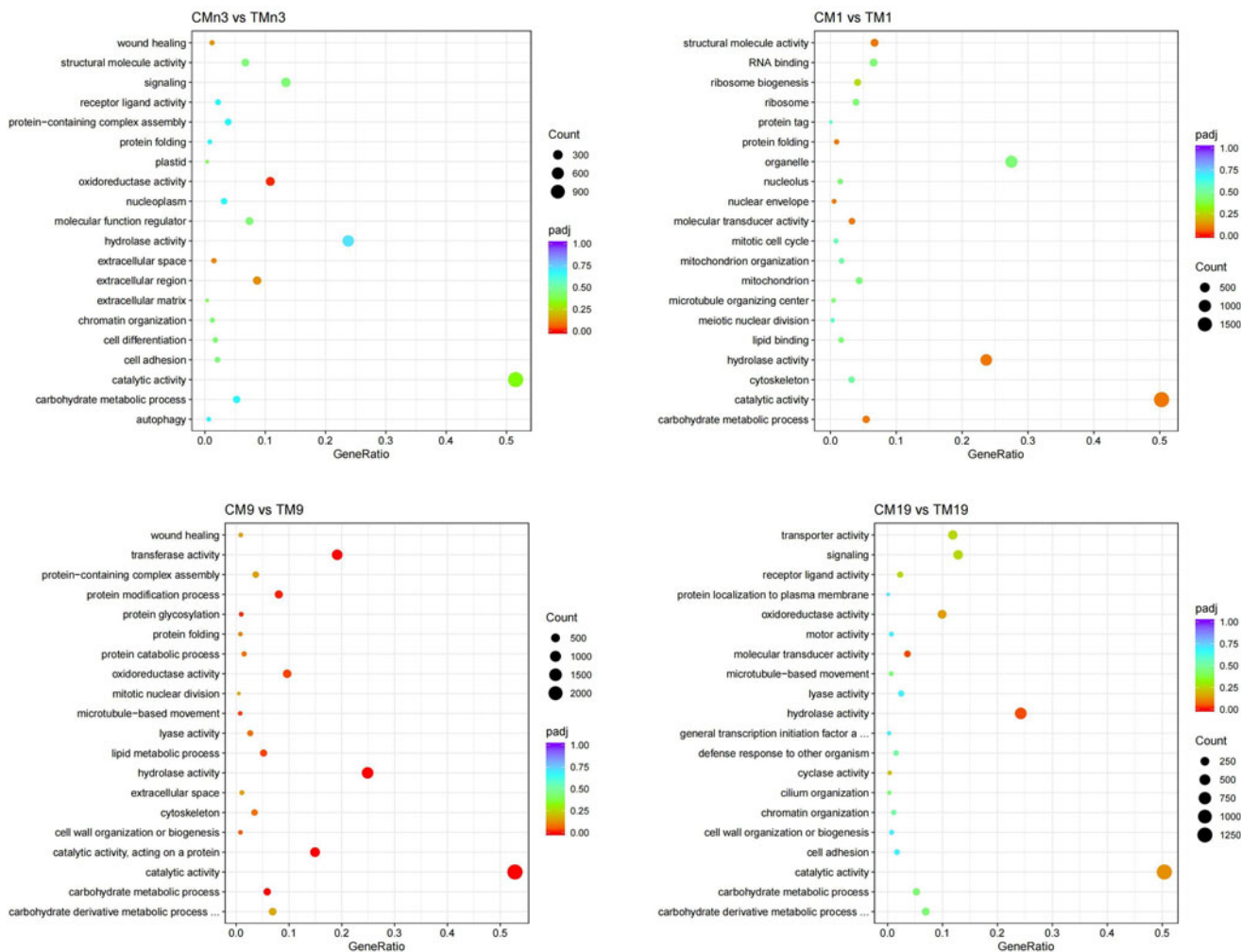


Figure 4. Dot plot of top 20 ranked GO terms of DEGs in different stages of male testis of *L. migratoria*. The figures represent the CMn3 vs. TMn3, CM1 vs. TM1, CM9 vs. TM9, CM19 vs. TM19, respectively. The vertical axis indicates GO terms and the horizontal axis represents the gene ratio. The size of dots indicates the number of genes in the GO term, and the colour of the dots corresponds to different P_{adj} ranges.

Analysis of DEGs in *L. migratoria* gonadal tissues of infected and uninfected *P. locustae*

Using the transcriptome data of uninfected *P. locustae* male and female gonadal tissues as controls, analysis of DEGs was performed. Upon infection with *P. locustae*, *L. migratoria* third-instar nymphs exhibited 2382 DEGs in female ovary tissues, with 1134 downregulated genes and 1248 upregulated genes; and 4957 DEGs in male testis tissues, with 2580 downregulated genes and 2377 upregulated genes. After nymphs eclosed into adults, the number of DEGs increased. Female locusts had the most DEGs at 1 day post-eclosion, with 7141 DEGs, including 3902 downregulated and 3239 upregulated genes. DEGs in male locusts continued to increase, peaking at 9 days post-eclosion with 11,245 DEGs, including 6412 downregulated and 4833 upregulated genes (fig. 1). Venn diagrams illustrated the overlap of DEGs among different comparison groups. After infection with *P. locustae*, there were 25 common DEGs in female groups (CFn3 vs. TFn3, CF1 vs. TF1, CF9 vs. TF9, CF19 vs. TF19) and 205 common DEGs in male groups (CMn3 vs. TMn3, CM1 vs. TM1, CM9 vs. TM9, CM19 vs. TM19) (fig. 2).

Significant enrichment analysis of DEGs in GO functions

GO functional annotation analysis was performed on DEGs in female ovary tissues. Results showed no significant enrichment in CFn3 vs. TFn3 and CF1 vs. TF1 groups. In the CF9 vs. TF9 group, DEGs were significantly enriched in ribosome (GO:0005840), oxidoreductase activity (GO:0016491), and ribosome biogenesis (GO:0042254), with 91, 191, and 90 differential genes, respectively ($P_{adj} < 0.05$). In the CF19 vs. TF19 group, DEGs were significantly enriched in transporter activity (GO:0005215), transmembrane transport (GO:0055085), external encapsulating structure (GO:0030312), and molecular transducer activity (GO:0060089), with 196, 165, 24, and 57 differential genes, respectively ($P_{adj} < 0.05$) (fig. 3).

GO functional annotation analysis of DEGs in male testis tissues showed significant enrichment in oxidoreductase activity (GO:0016491) in the CMn3 vs. TMn3 group, with 239 differential genes ($P_{adj} < 0.05$). In the CM1 vs. TM1 group, there was no significant enrichment. In the CM9 vs. TM9 group, DEGs were significantly enriched in various categories including catalytic activity (GO:0003824), catalytic activity, acting on a protein (GO:0140096), hydrolase activity (GO:0016787), carbohydrate metabolic process (GO:0005975), transferase activity (GO:0016740),

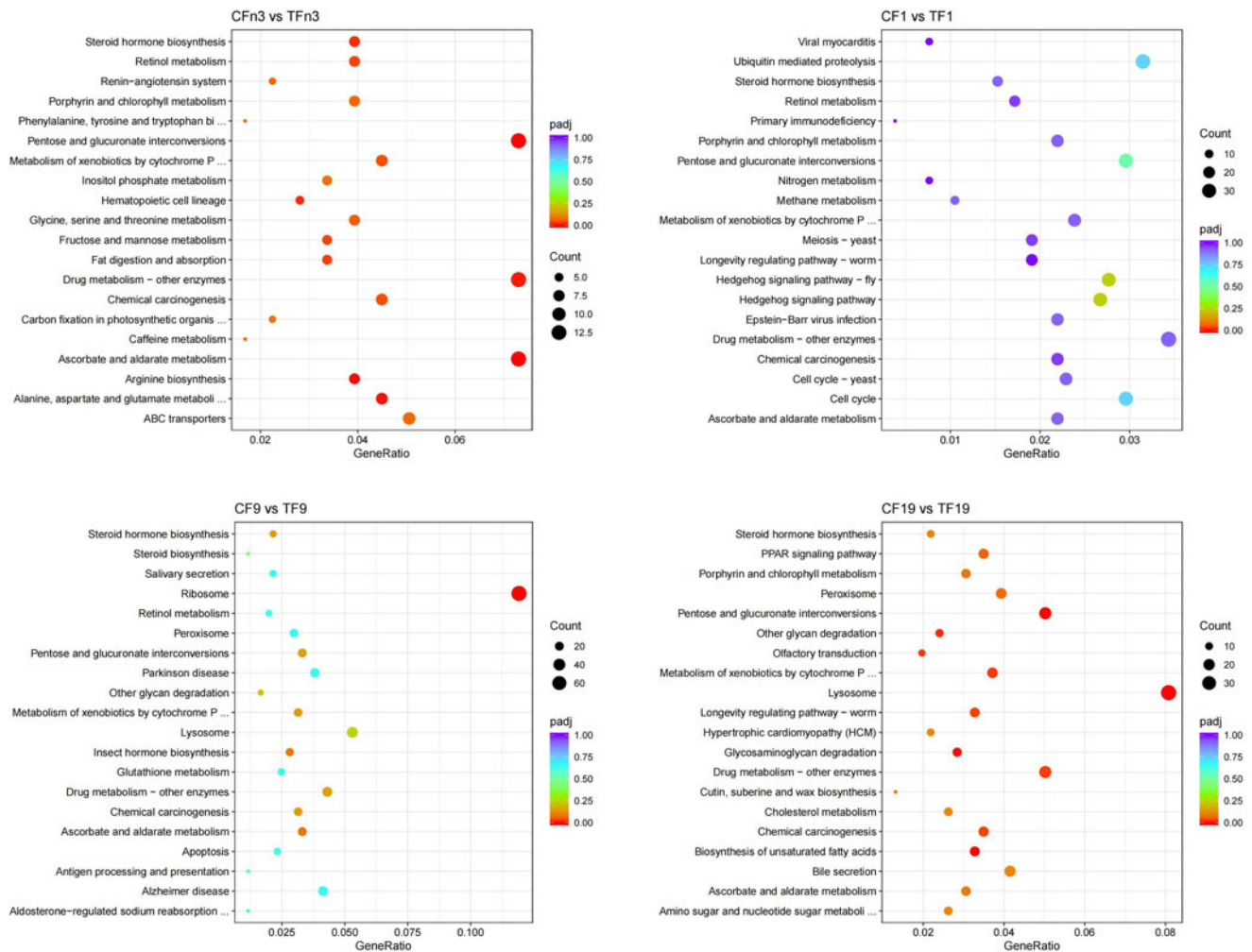


Figure 5. KEGG analysis of DEGs in different stages of female ovary of *L. migratoria*. The figures represent the KEGG pathway for the CFn3 vs. TFn3, CF1 vs. TF1, CF9 vs. TF9, CF19 vs. TF19, respectively. The vertical axis represents the pathway name, and the horizontal axis represents the gene ratio. The size of the dots indicates the number of genes in the pathway, and the colour of the dots corresponds to different P_{adj} ranges.

protein modification process (GO:0036211), protein glycosylation (GO:0006486), microtubule-based movement (GO:0007018), lipid metabolic process (GO:0006629), and oxidoreductase activity (GO:0016491), with 2458, 696, 1159, 274, 891, 376, 45, 36, 242, and 450 differential genes, respectively ($P_{adj} < 0.05$). In the CM19 vs. TM19 group, DEGs were significantly enriched in hydrolase activity (GO:0016787) and molecular transducer activity (GO:0060089), with 625 and 93 differential genes, respectively ($P_{adj} < 0.05$) (fig. 4).

Enrichment analysis of KEGG pathways for DEGs

Enrichment analysis of KEGG pathways for DEGs in female ovary tissues revealed significant enrichment in various metabolic pathways in different comparison groups. In the CFn3 vs. TFn3 group, DEGs were significantly enriched in pathways such as ascorbate and aldarate metabolism (ko00053), pentose and glucuronate interconversions (ko00040), arginine biosynthesis (ko00220), alanine, aspartate, and glutamate metabolism (ko00250), drug metabolism - other enzymes (ko00983), hematopoietic cell lineage (ko04640), steroid hormone biosynthesis (ko00140), fat digestion and absorption (ko04975), fructose and mannose

metabolism (ko00051), retinol metabolism (ko00830), chemical carcinogenesis (ko05204), and metabolism of xenobiotics by cytochrome P450 (ko00980). Differential gene counts ranged from 5 to 13 for these pathways ($P_{adj} < 0.05$). The CF1 vs. TF1 group showed no significant enrichment. In the CF9 vs. TF9 group, DEGs were significantly enriched only in the ribosome pathway (ko03010), with 72 differential genes ($P_{adj} < 0.05$). In the CF19 vs. TF19 group, DEGs were significantly enriched in pathways such as lysosome (ko04142), biosynthesis of unsaturated fatty acids (ko01040), pentose and glucuronate interconversions (ko00040), glycosaminoglycan degradation (ko00531), other glycan degradation (ko00511), olfactory transduction (ko04740), metabolism of xenobiotics by cytochrome P450 (ko00980), drug metabolism - other enzymes (ko00983), longevity regulating pathway - worm (ko04212), and chemical carcinogenesis (ko05204). Differential gene counts ranged from 9 to 37 for these pathways ($P_{adj} < 0.05$) (fig. 5).

For DEGs in male testis tissues, no significant enrichment was observed in the CMn3 vs. TMn3, CM9 vs. TM9, and CM19 vs. TM19 groups. However, in the CM1 vs. TM1 group, DEGs were significantly enriched in the spliceosome pathway (ko03040), with 59 differential genes ($P_{adj} < 0.05$) (fig. 6).

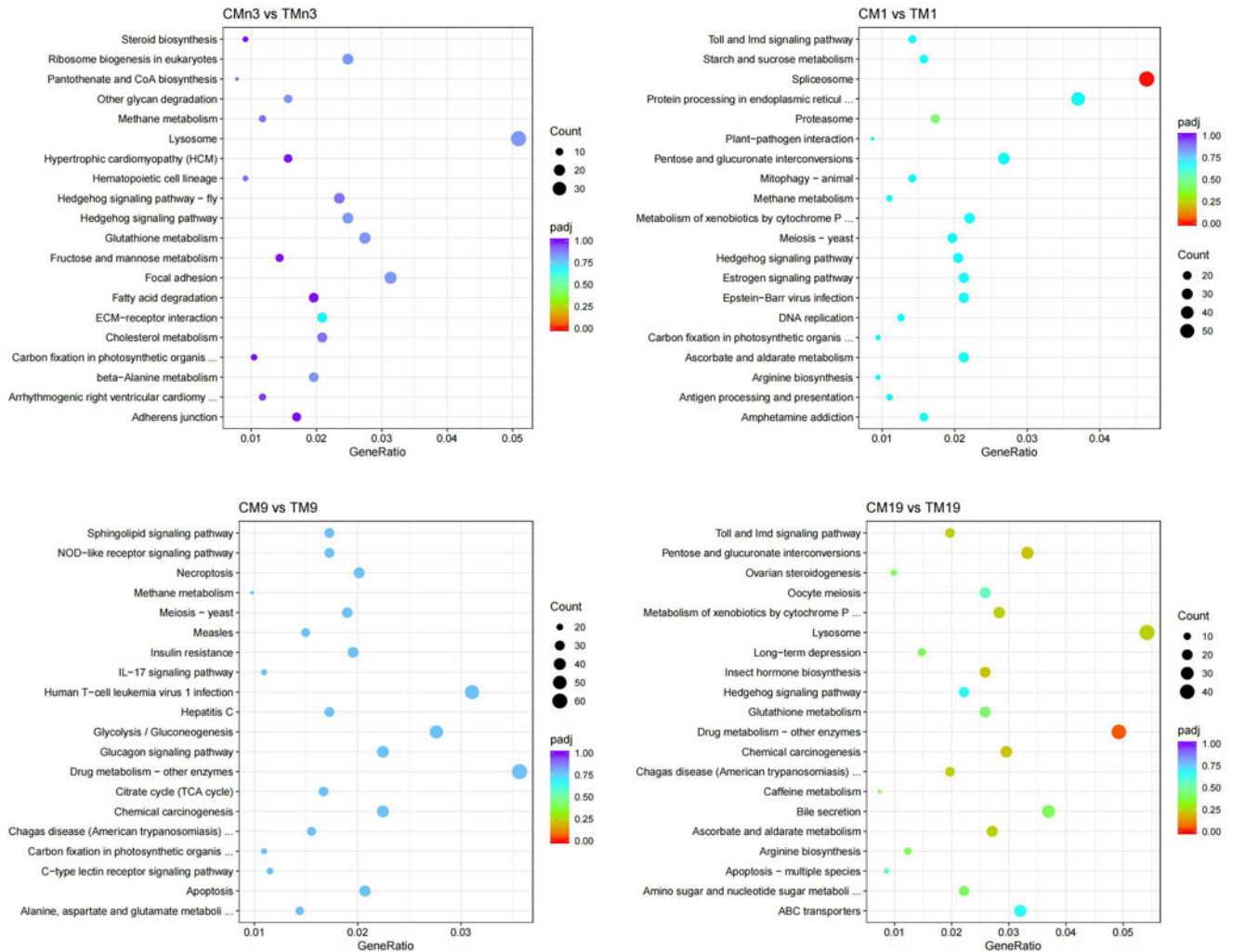


Figure 6. KEGG analysis of DEGs in different stages of male testis of *L. migratoria*. The figures represent the KEGG pathway for the CMn3 vs. TMn3, CM1 vs. TM1, CM9 vs. TM9, CM19 vs. TM19, respectively. The vertical axis represents the pathway name, and the horizontal axis represents the gene ratio. The size of the dots indicates the number of genes in the pathway, and the colour of the dots corresponds to different P_{adj} ranges.

The network of PPI of DEGs

To further explore the possible mechanisms of gonadal tissue of *L. migratoria* resistance to *P. locustae* infection, the putative 690 key DEGs belonging to the CF1 vs. TF1 group, 225 DEGs belonging to CF9 vs. TF9 group, 757 DEGs belonging to CM1 vs. TM1 group, 1140 DEGs belonging to CM9 vs. TM9 group were used to build PPI networks. As shown in the CF1 vs. TF1 group in fig. 7, immune-related genes, such as *ACSL*, *APC3*, *DNM1L*, *GNG13*, *PTPN11*, and *TIAM1*, were significantly downregulated, while reproductive-related gene, *NCOA2*, was significantly upregulated in female ovary at 1 day post-eclosion. Similar results were also observed in other groups. The results indicate that immune- and reproductive-related gene expression were regulated to meet the body's demands in different developmental stages after *P. locustae* infection.

Selection and qRT-PCR validation of immune- and reproductive-related genes in *L. migratoria* gonadal tissues

Based on functional annotation and enrichment analysis of DEGs, along with relevant literature, immune- and reproductive-related

DEGs were selected from the transcriptome data. These genes included *Transferrin (Tsf)*, *Hexamerin-like protein 1 (Hex1)*, *Apolipophorin-III (ApoLp-III)*, and others associated with immune regulation, phagocytosis, stress response, and reproductive regulation (table 2). qRT-PCR was performed to validate the expression levels of *Tsf*, *Hex1*, and *ApoLp-III*. *Tsf* showed significant upregulation in female ovary tissues at 1 and 19 days post-eclosion and significant downregulation at 9 days post-eclosion ($P < 0.05$) (fig. 8A). In male testis tissues, *Tsf* was significantly upregulated in all developmental stages ($P < 0.05$) (fig. 8B). *Hex1* exhibited significant upregulation in female ovary tissues at 1 and 19 days post-eclosion and in third-instar nymph male testis tissues ($P < 0.05$) (fig. 8C, D). However, its expression was significantly downregulated in male testis tissues at 1 day post-eclosion ($P < 0.05$) (fig. 8D). *ApoLp-III* showed significant upregulation in all developmental stages of both female ovary and male testis tissues ($P < 0.05$) (fig. 8E, F). A regression analysis was performed to evaluate and validate *Tsf*, *Hex1*, and *ApoLp-III* genes from RNA-Seq data using qRT-PCR. The results indicate a significant correlation coefficient ($R^2 = 0.71-0.99$) between RNA-Seq and qRT-PCR data expressed in log2FC (fig. S2). Correlation analysis revealed that the qRT-PCR

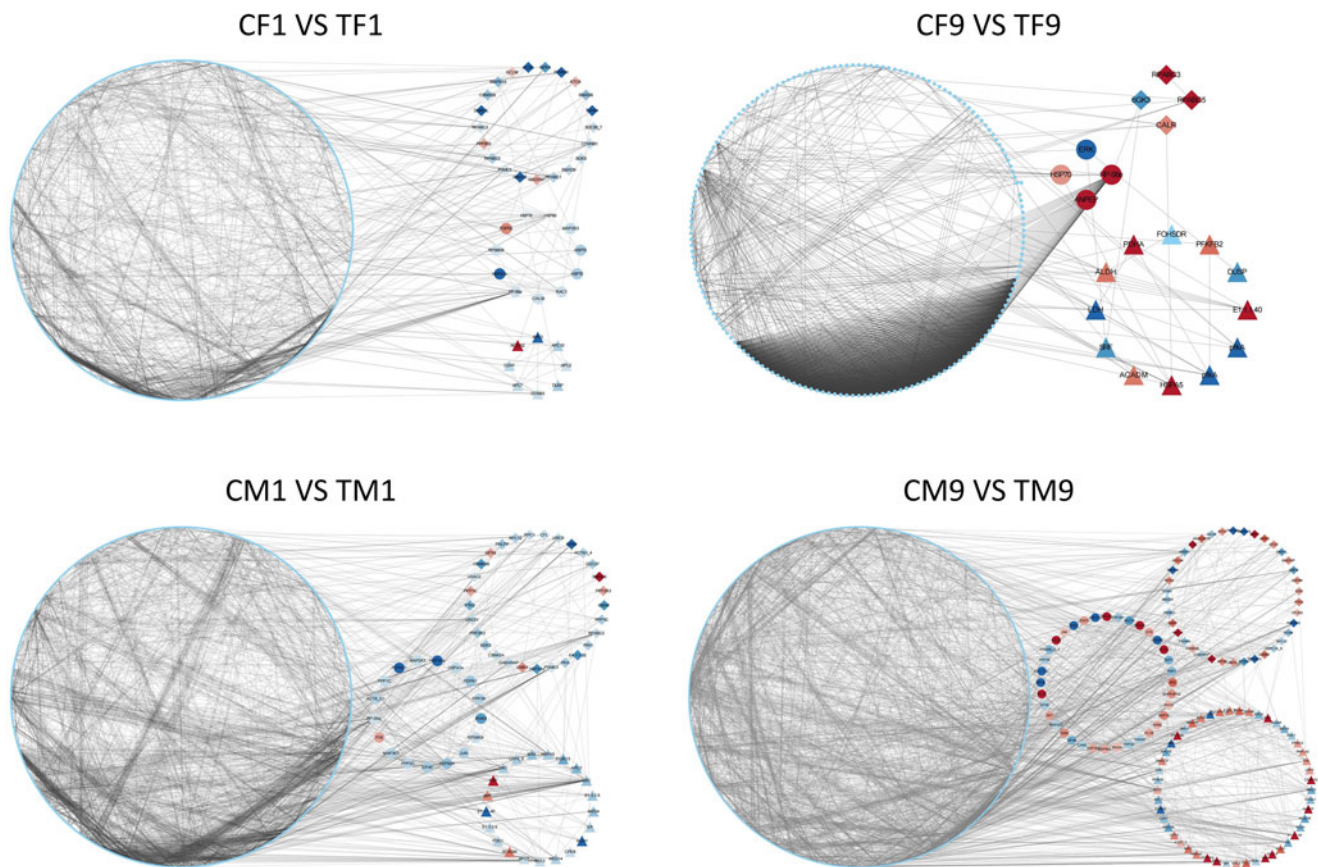


Figure 7. Network of PPI for DEGs. The figures represent the PPI analysis of DEGs in CF1 vs. TF1, CF9 vs. TF9, CM1 vs. TM1, CM9 vs. TM9, respectively. Nodes represent DEGs, and edges represent interactions between two DEGs. The rhombi represent DEGs related to immunity, the triangles represent DEGs related to reproduction; the circles represent DEGs related to immunity and reproduction. Red and blue represent an upward adjustment and a downward adjustment, respectively.

expression patterns of *Tsf*, *Hex1*, and *ApoLp-III* were all consistent with the RNA-Seq results, indicating that the RNA-Seq results were highly reliable.

Discussion

Interactions between pests and pathogens have long been a focal point in life sciences research. The gonads, as crucial reproductive organs in insects, play a pivotal role in the balance and regulation of immunity and reproduction when faced with pathogen infection, which ultimately determines the population dynamics of insects. Understanding the response of gonadal tissues to pathogen stress and elucidating the strategies of immunity and reproduction can facilitate the exploration of new pest control methods, especially from the perspective of reproductive regulation.

This study utilised high-throughput transcriptome sequencing to reveal that upon infection with *P. locustae*, differential gene expression in the ovaries of female *L. migratoria* primarily enriched in various immune-related GO categories and metabolic pathways, such as ribosome, oxidoreductase activity, transporter activity, etc. The differential gene expression in the testes of male locusts enriched in processes like catalytic activity, protein glycosylation, etc. This indicates that *P. locustae* infection modulates the basic metabolism and immune response of insect gonadal tissues (Aufauvre *et al.*, 2014; Zhang *et al.*, 2015b; Kurze *et al.*, 2016; Xu *et al.*, 2023).

The innate immune system plays a crucial role in insect resistance to pathogen infection. Previous studies have shown that insects such as *Bombyx mori* (Ma *et al.*, 2013) and *Apis mellifera* (Chaimanee *et al.*, 2012; Aufauvre *et al.*, 2014) enhance their immune systems by modulating pathways like the Toll signalling pathway, JAK/STAT signalling pathway, and expression of antimicrobial peptides upon pathogen infection. Similarly, upon infection with *Metarhizium acridum*, the expression of immune-related genes in *L. migratoria* also changes (Zhang *et al.*, 2015b). In this study, it was found that upon infection with *P. locustae*, the expression of immune-related genes in *L. migratoria* also changed. For instance, *Toll-like receptor* and *DSCAM2* were downregulated after *L. migratoria* third-instar nymphs were infected with *P. locustae*, while *DSCAM2*, *Defense*, *Lysozyme P*, *c-type Lysozyme* were gradually upregulated after eclosion at 1, 9, and 19 days. We might expect that *P. locustae* may evade the host's immune response by interfering with the expression of key genes in the host's immune system in the initial stages of infection. Subsequently, the body gradually upregulates the expression of immune-related genes to resist *P. locustae* infection.

In our study, qRT-PCR results revealed significant upregulation of *Tsf* in the testicular tissues of male *L. migratoria* upon infection with *P. locustae*. We speculate that organism can enhance resistance to *P. locustae* by upregulating *Tsf* expression to avoid oxidative stress damage caused by iron overload. Iron homeostasis plays a crucial role in the body's defence and stress

Table 2. Part of DEGs related to immunity and reproduction in gonadal tissue

Gene function	Genes	Gene number	Matched species	Length (bp)	E value	Identity (%)
Immune regulation and phagocytosis	<i>Transferrin (Tsf)</i>	Cluster-80928.60312	<i>L. migratoria</i>	2150	4.00×10^{-226}	99.74
	<i>Hexamerin-like protein 1 (Hex1)</i>	Cluster-80928.51085	<i>L. migratoria</i>	2340	2.90×10^{-52}	89.66
	<i>Apolipoprotein-III (Apolp-III)</i>	Cluster-80928.63301	<i>L. migratoria</i>	964	1.40×10^{-21}	98.21
	<i>Down syndrome cell adhesion molecule-like protein Dscam2 (DSCAM2)</i>	Cluster-80928.31127	<i>Blattella germanica</i>	2187	1.50×10^{-90}	37.92
	<i>proteinase inhibitor serpin (Serpin)</i>	Cluster-80928.79606	<i>L. migratoria</i>	464	1.90×10^{-72}	88.96
	<i>Toll-like receptor</i>	Cluster-80928.84875	<i>Gryllus bimaculatus</i>	627	1.40×10^{-14}	51.25
	<i>Toll-like receptor 2</i>	Cluster-80928.19844	<i>Cryptotermes secundus</i>	2201	2.90×10^{-30}	43.20
	<i>Defense</i>	Cluster-80928.56443	<i>L. migratoria</i>	1967	6.90×10^{-23}	88.89
	<i>Lysozyme P</i>	Cluster-80928.92100	<i>C. quinquefasciatus</i>	940	5.60×10^{-23}	42.02
	<i>c-type lysozyme</i>	Cluster-80928.19639	<i>L. migratoria</i>	1047	4.90×10^{-68}	97.56
Stress response	<i>Heat shock protein 70 (Hsp70)</i>	Cluster-80928.37489	<i>Oxya chinensis</i>	2486	0.00×10^0	87.03
	<i>Heat shock protein 90 (Hsp90)</i>	Cluster-80928.58562	<i>L. migratoria</i>	3338	1.40×10^{-20}	84.85
Reproductive regulation	<i>Juvenile hormone binding protein (JHBP)</i>	Cluster-80928.67710	<i>L. migratoria</i>	983	3.95×10^{-121}	97.70
	<i>Juvenile hormone esterase (JHE)</i>	Cluster-80928.59079	<i>Romalea microptera</i>	2538	2.00×10^{-240}	77.76
	<i>Juvenile hormone epoxide hydrolase 1-like (JHEH1)</i>	Cluster-80928.75447	<i>Zootermopsis nevadensis</i>	2186	1.50×10^{-143}	57.18
	<i>Juvenile hormone acid methyltransferase (JHAMT)</i>	Cluster-80928.62858	<i>Schistocerca gregaria</i>	2139	2.90×10^{-51}	42.19
	<i>Vitellogenin receptor (VgR)</i>	Cluster-80928.73361	<i>Athalia rosae</i>	595	4.20×10^{-16}	40.38

response mechanisms. Transferrin (Trf) is a key protein involved in maintaining iron homeostasis and participates in iron metabolism, oxidative stress defence, and innate immunity (Najera *et al.*, 2019; Weber *et al.*, 2020, 2022; Zafar *et al.*, 2022). Studies have shown that upon exposure to insecticide stress, mosquitoes like *Culex pipiens pallens* (Tan *et al.*, 2012), *Helicoverpa armigera* (Zhang *et al.*, 2015a), *Spodoptera littoralis* (Hamama *et al.*, 2016), and *L. migratoria* (Gao, 2016) exhibit upregulated expression of transferrin. Similarly, pathogen stress can induce the upregulation of host transferrin expression, thereby regulating iron homeostasis and transport (Desjardins *et al.*, 2015). For instance, in *Drosophila melanogaster*, transcription levels of *Transferrin* significantly increase after *Escherichia coli* infection, where it employs iron inhibition strategies to combat infection, a process dependent on nuclear factor- κ B, Toll, Imd, and other signalling pathways (Iatsenko *et al.*, 2020). Moreover, *Plutella xylostella* shows increased expression of *PxTrf* after treatment with *Staphylococcus aureus*, *E. coli*, and *Isaria cicadae* (Xu *et al.*, 2020). Simultaneously, interference with *PxTrf* expression significantly inhibits the formation of *P. xylostella* haemocyte nodules and enhances its sensitivity to *I. cicadae* (Xu *et al.*, 2020). In *A. mellifera*, infection with *Nosema ceranae* leads to iron deficiency

in the body and induces upregulation of *AmTsf* expression. Silencing *AmTsf* expression through RNAi alleviates iron loss, enhances honey bee immunity, and increases survival rates (Rodríguez-García *et al.*, 2021). This multifaceted role of transferrin in the immune response is evident across various studies.

In our study, *Hex1* was significantly upregulated in the ovarian tissues of female *L. migratoria* at 1 and 19 days post-eclosion upon infection with *P. locustae*. We speculate that females prioritise the upregulation of reproductive-related genes in response to immune and reproductive pressures, meeting the amino acid reserve demands for gamete development and gonadal maturation, thereby ensuring population reproduction. *Hexamerin* is another important functional protein involved in various life activities such as cuticle formation, hormone transport, lipid transportation, energy metabolism, diapause, metamorphosis, and plays a significant role in the immune response (Burmester, 2015; Janashia and Alaux, 2016; Lieb *et al.*, 2016; Cui *et al.*, 2019). *Circulifer haematoceps* exhibits upregulated expression of *Hexamerin* upon infection with *Spiroplasma citri* (Eliatout *et al.*, 2016). Similarly, treatment with organophosphate results in increased *Hexamerin* expression in *Culex quinquefasciatus* (Games *et al.*, 2016). Conversely, effective chlorofluorocarbon pesticide treatment downregulates *Hexamerin*

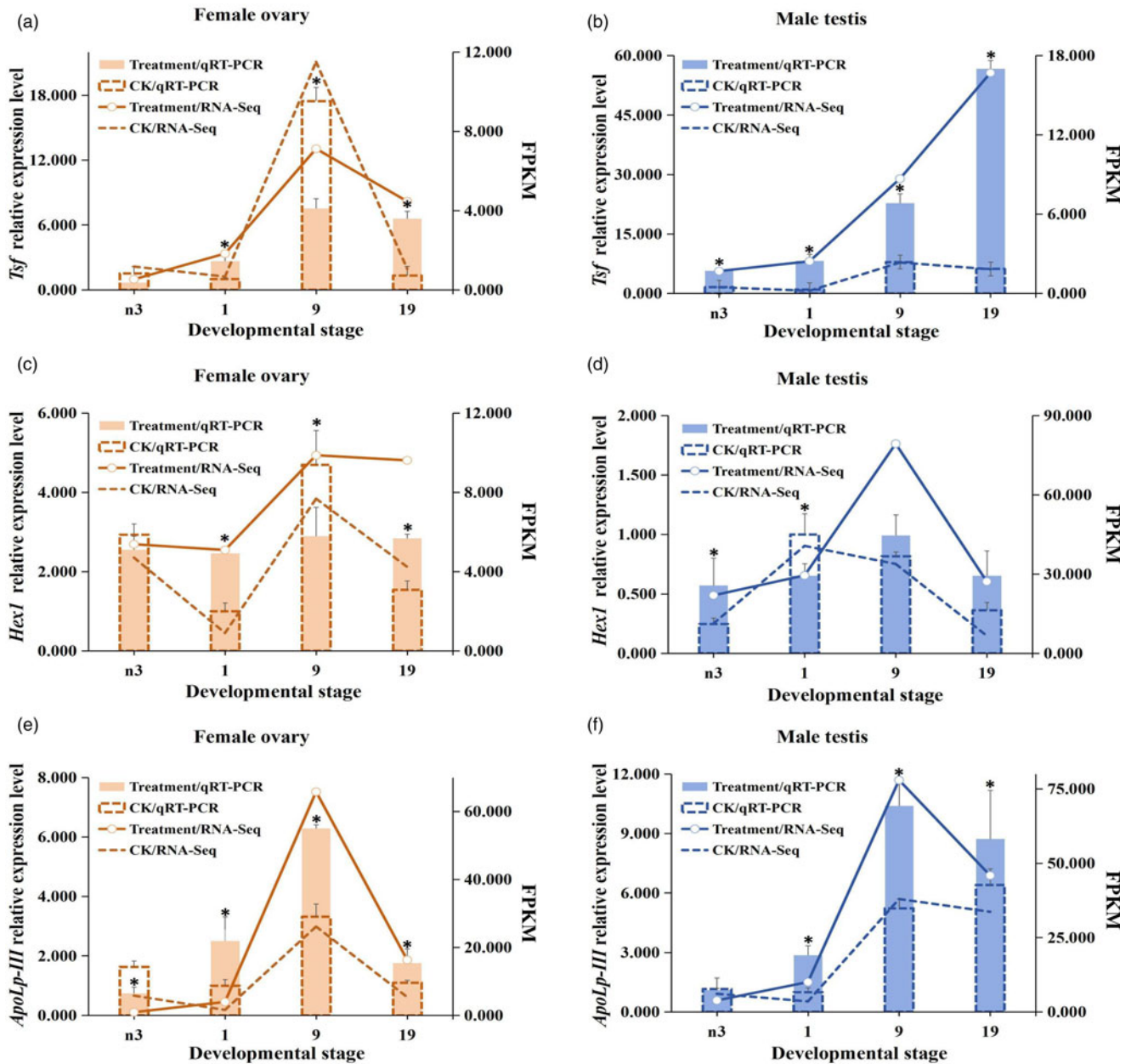


Figure 8. Relative expression levels of three unigenes, including *Tsf*, *Hex1*, and *ApoLp-III* among different stages of ovary and testis in *L. migratoria*. Columns and polylines indicate the relative expression levels of genes identified by qRT-PCR and RNA-Seq, respectively. *EF1 α -F* was used as an internal control. The details of the primers are shown in table S1. Data are expressed as mean \pm SE ($n = 3$). Asterisks above columns indicate statistically significant differences by one-way ANOVA with Duncan's test ($P < 0.05$). n3 indicates third-instar locust nymphs. 1, 9, and 19 indicate 1, 9, and 19 days adult after emergence, respectively.

expression in *Spodoptera exigua* larvae (Wang *et al.*, 2019b). This indicates differential regulation of *Hexamerin* expression under different stresses. In *L. migratoria*, stimulation with *E. coli* leads to a trend of first downregulation and then upregulation of *Hex1* and *Hex2* expression in fat bodies, while *Hex3* and *Hex4* show the opposite trend, suggesting that *Hexamerin* family genes have immune functions with possible mutual compensation effects among members (Zhang *et al.*, 2018). Injection of *Antheraea pernyi* larvae with *S. aureus*, *E. coli*, and *Candida albicans* leads to a sharp increase in *Ap-hexamerin* expression in fat bodies 12 h post-treatment, confirming the significant enhancement of phenoloxidase activity by *Ap-hexamerin* and its involvement in the early immune response of *A. pernyi* (Liu *et al.*, 2019). *Hexamerin* also

plays a crucial role in insect reproduction. Expression analysis of *AcHex-2* in 5th- and 12th-instar *Acrida cinerea* adults shows that it is predominantly expressed in the ovaries and testes, with significantly higher expression in the 12th instar compared to the 5th instar, indicating its tissue specificity and importance during reproduction (Dong *et al.*, 2015).

Our qRT-PCR results indicate a significant upregulation of *ApoLp-III* expression in the gonadal tissues of male and female *L. migratoria* at 1, 9, and 19 days post-eclosion after *P. locustae* infection, suggesting its involvement in the immune defence response of *L. migratoria* against *P. locustae*. Additionally, transcriptome results show upregulation of *Defense*, *Toll-like receptor*, and *Serpin* expression in the gonadal tissues of *L. migratoria* at 1,

9, and 19 days post-eclosion, suggesting the possible involvement of *ApoLp-III* in regulating key genes of the Toll and serine protease inhibitor pathways in the immune response of *L. migratoria*. Apolipoprotein plays a crucial role in lipid transport, lipoprotein metabolism, and innate immunity in insects, divided into ApoLp-I, ApoLp-II, and ApoLp-III (Browne *et al.*, 2014; Wen *et al.*, 2017). As a pattern recognition molecule, ApoLp-III participates in the immune response and phagocytosis process of the organism by activating functional protein activity, thereby enhancing the antibacterial and antifungal capabilities (Zdybicka-Barabas *et al.*, 2015; Wijeratne and Weers, 2019; Sączek *et al.*, 2020). Studies have shown significant changes in ApoLp-III levels in various insects such as *Apis cerana* (Kim and Jin, 2015), *Actias selene* Hübner (Qian *et al.*, 2016), *Galleria mellonella* (Iwański and Andrejko, 2023), and *Spodoptera litura* (Vengateswari and Shivakumar, 2023) upon pathogen infection, demonstrating its antimicrobial activity and importance in the response to pathogen stress. In *Tenebrio molitor*, silencing of *TmApoLp-III* expression enhances larval sensitivity to *Listeria monocytogenes* (Patnaik *et al.*, 2015). Additionally, induction of *ScApoLp-III* expression is observed in the gut and fat bodies of *Samia cynthia ricini* upon *S. aureus* infection, while it is downregulated upon *Pseudomonas aeruginosa* induction (Yu *et al.*, 2018). Recombinant *ScApoLp-III* can bind to *E. coli*, *P. aeruginosa*, *S. aureus*, and *Bacillus subtilis*, strongly inhibiting the proliferation of *E. coli* and *P. aeruginosa* (Yu *et al.*, 2018). Studies have also shown that upon infection with *Beauveria bassiana*, *BmApoLp-III* expression is upregulated in *B. mori* larvae, and recombinant *BmApoLp-III* protein significantly inhibits the proliferation of *B. bassiana*, delaying the onset of symptoms and death in infected larvae (Wu *et al.*, 2021). Moreover, *BmApoLp-III* can regulate the expression of genes related to the Toll, JAK/STAT, and Imd signalling pathways, promoting the expression of immune effectors (Wu *et al.*, 2021).

Through transcriptomic analysis, our study reveals significant changes in basic metabolism and immune response processes in the gonadal tissues of male and female *L. migratoria* after *P. locustae* infection, including amino acid metabolism, carbohydrate metabolism, lipid metabolism, and the involvement of genes such as *Transferrin*, *Hexamerin*, *Apolipoprotein*, Toll signalling pathway regulatory proteins, *Heat shock proteins*, Juvenile hormone-related proteins and enzymes, and *Vitellogenin receptor* in the immune and reproductive balance of gonadal tissues. These findings are crucial for further elucidating the possible mechanisms underlying the response of *L. migratoria* gonadal tissues to *P. locustae* infection, identifying optimal pest control targets, and enhancing the efficacy of *P. locustae* against locusts.

Supplementary material. The supplementary material for this article can be found at <https://doi.org/10.1017/S0007485324000592>.

Availability of data and materials. All data generated or analysed during this study are included in this article.

Author contributions. Xuewei Kong carried out the studies, participated in collecting data, in acquisition, analysis, or interpretation of data, performed the statistical analysis, participated in experimental design, drafted the manuscript, and participated in paper review and editing. Xinrui Guo participated in collecting data, in acquisition, analysis, or interpretation of data, performed the statistical analysis. Hui Liu and Huihui Zhang participated in collecting data. Hongxia Hu, Jun Lin, Wangpeng Shi, Rong Ji, and Roman Jashenko participated in paper review and editing. Han Wang participated in funding acquisition, project administration, supervision, and experimental design, performed the statistical analysis, drafted the manuscript, and participated in paper review and editing.

Financial support. This work was supported by Special Project of Innovation Environment (Talent and Base) Construction in Xinjiang Uygur Autonomous Region (grant number 2022D04002); Natural Science Foundation in Xinjiang Uygur Autonomous Region (grant number 2021D01A124); Xinjiang Uygur Autonomous Region Science and Technology support Xinjiang Project plan (mandatory) project (grant number 2022E02007); and Tianshan Talent Training Program (grant number TSYCLJ0016).

Competing interests. None.

References

- Aufauvre J, Misme-Aucouturier B, Vigués B, Texier C, Delbac F and Blot N (2014) Transcriptome analyses of the honeybee response to *Nosema ceranae* and insecticides. *PLoS ONE* **9**, e91686.
- Browne N, Surlis C and Kavanagh K (2014) Thermal and physical stresses induce a short-term immune priming effect in *Galleria mellonella* larvae. *Journal of Insect Physiology* **63**, 21–26.
- Budischak SA, Hansen CB, Caudron Q, Garnier R, Kartzinel TR, Pelczar I, Cressler CE, Leeuwen A and Graham AL (2018) Feeding immunity: physiological and behavioral responses to infection and resource limitation. *Frontiers in Immunology* **8**, 1914.
- Burmester T (2015) Expression and evolution of hexamerins from the tobacco hornworm, *Manduca sexta*, and other Lepidoptera. *Insect Biochemistry and Molecular Biology* **62**, 226–234.
- Chaimanee V, Chantawannakul P, Chen YP, Evans JD and Pettis JS (2012) Differential expression of immune genes of adult honey bee (*Apis mellifera*) after inoculated by *Nosema ceranae*. *Journal of Insect Physiology* **58**, 1090–1095.
- Chen JX, Shen J, Song DL, Zhang L and Yan YH (2002) Effect of *Nosema locustae* on the content of vitellogenin of *Locusta migratoria manilensis*. *Acta Entomologica Sinica* **45**, 170–174.
- Chen LX, Gao XK, Li RT, Zhang LM, Huang R, Wang LQ, Song Y, Xing ZZ, Liu T, Nie XN, Nie FY, Hua S, Zhang ZH, Wang F, Ma RLZ and Zhang L (2020) Complete genome of a unicellular parasite (*Antonospora locustae*) and transcriptional interactions with its host locust. *Microbial Genomics* **6**, mgen000421.
- Cui DN, Tu XB, Hao K, Aftab R, Chen J, Mark M and Zhang ZH (2019) Identification of diapause-associated proteins in migratory locust, *Locusta migratoria* L. (Orthoptera: Acridoidea) by label-free quantification analysis. *Journal of Integrative Agriculture* **18**, 2579–2588.
- Dakhl WH, Latchininsky AV and Jaronski ST (2019) Efficacy of two entomopathogenic fungi, *Metarhizium brunneum*, Strain F52 alone and combined with *Paranosema locustae* against the migratory grasshopper, *Melanoplus sanguinipes*, under laboratory and greenhouse conditions. *Insects* **10**, 94.
- Davidson NM and Oshlack A (2014) Corset: enabling differential gene expression analysis for de novo assembled transcriptomes. *Genome Biology* **15**, 410.
- Desjardins CA, Sanscrainte ND, Goldberg JM, Heiman D, Young S, Zeng QD, Madhani HD, Becnel JJ and Cuomo CA (2015) Contrasting host-pathogen interactions and genome evolution in two generalist and specialist microsporidian pathogens of mosquitoes. *Nature Communications* **6**, 7121.
- Dong LJ, Zhang XH, Li YL, Lu SS and Yin H (2015) Cloning and expression analysis of a hexamerin gene from *Acrida cinerea* (Acridoidea: Acrididae). *Journal of Agricultural Science and Technology* **17**, 78–84.
- Eliatout R, Dubrana MP, Vincent-Monégat C, Vallier A, Braquart-Varnier C, Poirie M, Saillard C, Heddi A and Arricau-Bouvery N (2016) Immune response and survival of *Circulifer haematocaps* to *Spiroplasma citri* infection requires expression of the gene *hexamerin*. *Developmental and Comparative Immunology* **54**, 7–19.
- Games PD, Alves SN, Katz BB, Tomich JM and Serrao JE (2016) Differential protein expression in the midgut of *Culex quinquefasciatus* mosquitoes induced by the insecticide temephos. *Medical and Veterinary Entomology* **30**, 253–263.
- Gao HL (2016) Effects of imidacloprid treatment on gene expression related to detoxification and defense in *Locusta migratori* (thesis). Nanjing Agricultural University.

- Grabherr MG, Haas BJ, Yassour M, Levin JZ, Thompson D, Amit I, Adiconis X, Lin F, Raychowdhury R, Zeng QD, Chen ZH, Mauceli E, Hacohen N, Gnirke A, Rhind N, Palma FD, Birren BW, Nusbaum C, Lindblad-Toh K, Friedman N and Regev A (2011) Full-length transcriptome assembly from RNA-Seq data without a reference genome. *Nature Biotechnology* **29**, 644–652.
- Hamama HM, Hussein MA, Fahmy AR, Fergani YA, Mabrouk AM and Farghaley SF (2016) A transferrin fragment isolated from the Egyptian cotton leaf worm, *Spodoptera littoralis* (Boisduval) (Lepidoptera: Noctuidae) in response to two commercial bioinsecticides. *Egyptian Journal of Biological Pest Control* **26**, 59–64.
- Hu YW, Wang SH, Tang Y, Xie GQ, Ding YJ, Xu QY, Tang B, Zhang L and Wang SG (2022) Suppression of yolk formation, oviposition and egg quality of locust (*Locusta migratoria manilensis*) infected by *Paranosema locustae*. *Frontiers in Immunology* **13**, 848267.
- Iatsenko I, Marra A, Boquete JP, Peña J and Lemaitre B (2020) Iron sequestration by transferrin I mediates nutritional immunity in *Drosophila melanogaster*. *Proceedings of the National Academy of Sciences of the United States of America* **117**, 7317–7325.
- Iwański B and Andrejko M (2023) Changes in the apolipoprotein III in *Galleria mellonella* larvae treated with *Pseudomonas aeruginosa* exotoxin A. *Journal of Insect Physiology* **149**, 104536.
- Janashia I and Alaux C (2016) Specific immune stimulation by endogenous bacteria in honey bees (Hymenoptera: Apidae). *Journal of Economic Entomology* **109**, 1474–1477.
- Kim BY and Jin BR (2015) Apolipoprotein III from honeybees (*Apis cerana*) exhibits antibacterial activity. *Comparative Biochemistry and Physiology Part B: Biochemistry and Molecular Biology* **182**, 6–13.
- Kurze C, Dosselli R, Grassl J, Le Conte Y, Kryger P, Baer B and Moritz RFA (2016) Differential proteomics reveals novel insights into *Nosema*–honey bee interactions. *Insect Biochemistry and Molecular Biology* **79**, 42–49.
- Lieb B, Ebner B and Hartmut K (2016) cDNA sequences of two arylphorin subunits of an insect biliprotein: phylogenetic differences and gene duplications during evolution of hexamerins – implications for hexamer formation. *Journal of Experimental Zoology Part B: Molecular and Developmental Evolution* **326**, 136–148.
- Liu CB, Zhu JY, Ma JJ, Zhang JH, Wang XL and Zhang R (2019) A novel hexamerin with an unexpected contribution to the prophenoloxidase activation system of the Chinese oak silkworm, *Antheraea pernyi*. *Archives of Insect Biochemistry and Physiology* **103**, e21648.
- Liu H, Wei XJ, Ye XF, Zhang HH, Yang K, Shi WP, Zhang JR, Jashenko R, Ji R and Hu HX (2023) The immune response of *Locusta migratoria manilensis* at different times of infection with *Paranosema locustae*. *Archives of Insect Biochemistry and Physiology* **114**, e22055.
- Love MI, Huber W and Anders S (2014) Moderated estimation of fold change and dispersion for RNA-Seq data with DESeq2. *Genome Biology* **15**, 550.
- Lv MY, Mohamed AA, Zhang LW, Zhang PF and Zhang L (2016) A family of CS β defensins and defensin-like peptides from the migratory locust, *Locusta migratoria*, and their expression dynamics during mycosis and nosemosis. *PLoS ONE* **11**, e0161585.
- Ma ZG, Li CF, Pan GQ, Li ZH, Han B, Xu JS, Lan XQ, Chen J, Yang DL, Chen QM, Sang Q, Ji XC, Li T, Long MX and Zhou ZY (2013) Genome-wide transcriptional response of silkworm (*Bombyx mori*) to infection by the microsporidian *Nosema bombycis*. *PLoS ONE* **8**, e84137.
- Mao XZ, Cai T, Olyarchuk JG and Wei LP (2005) Automated genome annotation and pathway identification using the KEGG Orthology (KO) as a controlled vocabulary. *Bioinformatics (Oxford, England)* **21**, 3787–3793.
- Najera DG, Coca M, Nutsch KE and Gorman MJ (2019) Characterization of a membrane-bound insect transferrin. *The FASEB Journal* **33**, 795.11.
- Panek J, El Alaoui H, Mone A, Urbach S, Demetree E, Texier C, Brun C, Zanzoni A, Peyretailade E, Parisot N, Lerat E, Peyret P, Delbac F and Biron DG (2014) Hijacking of host cellular functions by an intracellular parasite, the microsporidian *Anncaliia algerae*. *PLoS ONE* **9**, e100791.
- Patnaik BB, Patnaik HH, Park KB, Jo YH, Le YS and Han YS (2015) Silencing of apolipoprotein-III causes abnormal adult morphological phenotype and susceptibility to *Listeria monocytogenes* infection in *Tenebrio molitor*. *Entomological Research* **45**, 116–121.
- Qian C, Wang F, Zhu BJ, Wei GQ, Li S, Liu CL and Wang L (2016) Identification and characterization of an *Apolipoprotein-III* gene from *Actias selene* Hübner (Lepidoptera: Saturniidae). *Journal of Asia-Pacific Entomology* **19**, 103–108.
- Rodríguez-García C, Heerman MC, Cook SC, Evans JD, DeGrandi-Hoffman G, Banmeke O, Zhang Y, Huang SK, Hamilton M and Chen YP (2021) Transferrin-mediated iron sequestration suggests a novel therapeutic strategy for controlling *Nosema* disease in the honey bee, *Apis mellifera*. *PLoS Pathogens* **17**, e1009270.
- Schwenke RA, Lazzaro BP and Wolfner MF (2016) Reproduction-immunity trade-offs in insects. *Annual Review of Entomology* **61**, 239–256.
- Shang F, Niu JZ, Ding BY, Zhang Q, Ye C, Zhang W, Smagghe G and Wang JJ (2018) Vitellogenin and its receptor play essential roles in the development and reproduction of the brown citrus aphid, *Aphis (Toxoptera) citricidus*. *Insect Molecular Biology* **27**, 221–233.
- Stączek S, Zdybicka-Barabas A, Wiater A, Pleszczyńska M and Cytryńska M (2020) Activation of cellular immune response in insect model host *Galleria mellonella* by fungal α -1,3-glucan. *Pathogens and Disease* **78**, ftaa062.
- Tan WB, Wang X, Cheng P, Liu LJ, Wang HF, Gong MQ, Quan X, Gao HG and Zhu CL (2012) Cloning and overexpression of transferrin gene from cypermethrin-resistant *Culex pipiens pallens*. *Parasitology Research* **110**, 939–959.
- Trapnell C, Williams BA, Pertea G, Mortazavi A, Kwan G, van Baren MJ, Salzberg SL, Wold BJ and Pachter L (2010) Transcript assembly and abundance estimation from RNA-Seq reveals thousands of new transcripts and switching among isoforms. *Nature Biotechnology* **28**, 511–515.
- Vengateswari G and Shivakumar MS (2023) Isolation identification and molecular characterization of immune defense proteins from *Bacillus thuringiensis* challenged *Spodoptera litura* (Lepidoptera: Noctuidae) larvae. *Research Journal of Biotechnology* **18**, 112–117.
- Wang SH, Liu XJ, Xia ZY, Xie GQ, Tang B and Wang SG (2019a) Transcriptome analysis of the molecular mechanism underlying immunity and reproduction trade-off in *Locusta migratoria* infected by *Micrococcus luteus*. *PLoS ONE* **14**, e0211605.
- Wang SY, Hu B, Wei Q and Su JY (2019b) Cloning and characterization of hexamerin in *Spodoptera exigua* and the expression response to insecticide exposure. *Journal of Asia-Pacific Entomology* **22**, 602–610.
- Weber JJ, Park YJ and Gorman M (2020) Secreted insect transferrin-I with strong and reversible iron-binding has potentially tissue specific roles in immunity and iron transport. *The FASEB Journal* **34**, 1.
- Weber JJ, Brummett LM, Coca ME, Tabunoki H, Kanost MR, Ragan EJ, Park Y and Gorman MJ (2022) Phenotypic analyses, protein localization, and bacteriostatic activity of *Drosophila melanogaster* transferrin-I. *Insect Biochemistry and Molecular Biology* **147**, 103811.
- Wen DH, Luo H, Li TN, Wu CF, Zhang JH, Wang XL and Zhang R (2017) Cloning and characterization of an insect apolipoprotein (apolipoprotein-II/I) involved in the host immune response of *Antheraea pernyi*. *Developmental and Comparative Immunology* **77**, 221–228.
- Wijeratne T and Weers PMM (2019) Lipid-bound apoLp-III is less effective in binding to lipopolysaccharides and phosphatidylglycerol vesicles compared to the lipid-free protein. *Molecular and Cellular Biochemistry* **458**, 61–70.
- Wu WM, Lin S, Zhao Z, Su Y, Li RL, Zhang ZD and Guo XJ (2021) *Bombyx mori* apolipoprotein-III inhibits *Beauveria bassiana* directly and through regulating expression of genes relevant to immune signaling pathways. *Journal of Invertebrate Pathology* **184**, 107647.
- Xu HH, Hao ZP, Wang LF, Li SJ, Guo YR and Dang XL (2020) Suppression of transferrin expression enhances the susceptibility of *Plutella xylostella* to *Isaria cicadae*. *Insects* **11**, 281.
- Xu X, Wu YJ, Yu B, Meng XZ, Chen J, Liu ZW, Zhong YJ and Pan GQ (2023) Transcriptome and immune-related gene function analyses of *Antheraea pernyi* (Lepidoptera: Saturniidae) eggs infected by *Nosema pernyi*. *Acta Entomologica Sinica* **66**, 1560–1569.
- Yao Q, Xu S, Dong YZ, Que YL, Quan LF and Chen BX (2018) Characterization of vitellogenin and vitellogenin receptor of *Conopomorpha sinensis* Bradley and their responses to sublethal concentrations of insecticide. *Frontiers in Physiology* **9**, 1250.

- Young MD, Wakefield MJ, Smyth GK and Oshlack A** (2010) Gene ontology analysis for RNA-Seq: accounting for selection bias. *Genome Biology* **11**, R14.
- Yu HZ, Wang J, Zhang SZ, Toufееq S, Li B, Li Z, Yang LA, Hu P and Xu JP** (2018) Molecular characterisation of *Apolipophorin-III* gene in *Samia cynthia ricini* and its roles in response to bacterial infection. *Journal of Invertebrate Pathology* **159**, 61–70.
- Zafar J, Huang JL, Xu XX and Jin FL** (2022) Analysis of long non-coding RNA-mediated regulatory networks of *Plutella xylostella* in response to *Metarhizium anisopliae* infection. *Insects* **13**, 916.
- Zdybicka-Barabas A, Sowa-Jasilek A, Stączek S, Jakubowicz T and Cytryńska M** (2015) Different forms of apolipophorin III in *Galleria mellonella* larvae challenged with bacteria and fungi. *Peptides* **68**, 105–112.
- Zhang L and Lecoq M** (2021) *Nosema locustae* (Protozoa, Microsporidia), a biological agent for locust and grasshopper control. *Agronomy* **11**, 711.
- Zhang L, Shang Q, Lu Y, Zhao Q and Gao X** (2015a) A transferrin gene associated with development and 2-tridecanone tolerance in *Helicoverpa armigera*. *Insect Molecular Biology* **24**, 155–166.
- Zhang W, Chen JH, Keyhani NO, Zhang ZY, Li S and Xia YX** (2015b) Comparative transcriptomic analysis of immune responses of the migratory locust, *Locusta migratoria*, to challenge by the fungal insect pathogen, *Metarhizium acridum*. *BMC Genomics* **16**, 867.
- Zhang Z, Jiao LL, He K and Yin H** (2018) Expression and immune functional analysis of *hexamerin* gene family in *Locusta migratoria* (Acridoidea: Oedipodidae). *Journal of Agricultural Science and Technology* **20**, 45–51.
- Zhang H, Xu N, Cao LR, Wang R and Zhang K** (2023a) Review on research and utilization of microbial pesticides in China. *Chinese Journal of Pesticide Science* **25**, 769–778.
- Zhang HH, Yang K, Wang H, Liu H, Shi WP, Kabak I, Ji R and Hu HX** (2023b) Molecular and biochemical changes in *Locusta migratoria* (Orthoptera: Acrididae) infected with *Paranosema locustae*. *Journal of Insect Science* **23**, 1–8.